

# An Experimental Study of Crystallization and Crystal Growth of Methane Hydrates from Melting Ice\*

M. J. HWANG, D. A. WRIGHT, A. KAPUR, and G. D. HOLDER

Chemical and Petroleum Engineering Department, University of Pittsburgh, Pittsburgh, PE 15261, U.S.A.

(Received: 3 February 1988; in final form: 2 July 1988)

**Abstract.** An experiment with well defined gas–water interfacial surface area was developed to study the crystallization and crystal growth of methane hydrates. Measurable formation rates were observed only when melting ice was involved. No hydrates nucleated from liquid water or from non–melting ice. It is concluded that melting ice, which like hydrate water is hydrogen-bonded, provides a template for hydrate nucleation as well as providing a heat sink for absorbing the heat of formation during hydrate growth. The experiment was conducted in the absence of mixing so that hydrate crystals grew under quiescent conditions.

**Key words.** Clathrates, gas hydrates, kinetics, crystal growth.

## 1. Introduction

Gas hydrates belong to the family of nonstoichiometric inclusion compounds called clathrates. They are formed by the engagement of gases of small molecular diameters in the interstices of a hydrogen-bonded water lattice, and are similar in physical appearance to opaque ice crystals. These crystal lattices exhibit two structures, known as structure I and structure II. The topological feature common to both structures is the pentagonal dodecahedra, which pack into two different lattices – namely 12 Å cubic (space group  $Pm3n$ ) of Structure I and 17 Å cubic (space group  $Fd3m$ ) of Structure II. Early studies of hydrates were directed towards preventing their formation in natural gas pipelines, but discoveries of natural gas hydrates in arctic regions and under the ocean floor [1, 2] has stimulated interest in their study as a potential source of clean energy. Several comprehensive publications, covering nearly every aspect of gas hydrate history and nature, include works by Davidson [3], Finjord [4], and Holder *et al.* [5].

Although many investigators have studied the nature and thermodynamic properties of gas hydrates, a vast amount of physical, kinetic, and transport information on their formation and dissociation is still unknown. Such information is needed in order to develop realistic models for the way in which hydrates form in the earth. Previous investigations involve hydrate formation from either water or ice crystals, usually under well mixed conditions, with the primary system variables being temperature, pressure, and mixing [6, 7, 8]. The specific hydrate formation rate, however, was typically not measured as a function of the gas–water or gas–ice interfacial surface area. In addition, the interfacial surface area was created either by bubbling gas through water, or by mechanical agitation, and therefore the results may distort the determination of the conditions at which *in situ* hydrate

\* Dedicated to Dr D. W. Davidson in honor of his great contributions to the sciences of inclusion phenomena.

crystallization takes place. The formation of hydrate under dynamic conditions makes it difficult to study the morphology of hydrate crystals. In light of this, the purpose of this work was to measure the growth rate of methane hydrates from a geometrically well defined interfacial surface and under static conditions. In the absence of mixing, the true macroscopic crystal structure should be preserved during the enclathration process. The results may be useful in understanding the rates of hydrate formation in the earth, and subsequently in investigating the geological migration/formation histories of hydrate fields caused by changing temperature regimes.

## 2. Factors Affecting the Rate of Formation

A general chemical formula describing hydrate formation from a gas, or liquefied gas, and water is:



The coefficient  $\eta_h$  is called the hydrate number which is defined as the ratio of water molecules to gas molecules in the hydrate structure. To form hydrates, the pressure must be above the equilibrium dissociation pressure (the pressure at which the hydrates dissociate into gas and water). In fact, a high pressure driving force is required for measurable hydrate formation rates [9]. Makogon [1] suggested that the hydrate formation is an interfacial phenomenon, and hence high concentrations of hydrate forming species (gas and water) are required at the interface regardless of which of the three phases of water (liquid, solid or vapor) the hydrates are formed from.

Temperature is also important, primarily around the ice point. Above 0°C, the gas combines with liquid water and crystallization normally cannot be initiated in the bulk phase due to the low solubility of the gas in the bulk phase. In addition, hydrate formation is an exothermic process; heat is released as a result of phase change during crystallization. This heat tends to increase the temperature at the interface where the hydrates are being formed. This effect is greater for hydrate formation from liquid water than it is for formation from ice crystals since the heat of formation is partially absorbed by the melting ice crystals. In both cases, the heat must be removed from the interface quickly enough for hydrate crystals to be thermodynamically stable. Stirring of prenucleated systems provides the necessary heat transfer, enhances the dissolution of gas, and increases gas–water interfacial area. Barrer and coworkers [6, 10] and Falabella [11] studied the hydrate formation rates of different gases from very fine ice crystals at sub-atmospheric pressure and low temperatures (as low as –183°C). They found that at temperatures above –78°C the formation rates of some hydrates are slower and in certain cases (ice at –30° and –20°C) no formation of single hydrate was observed. Falabella suggested that at very low temperatures the high surface mobility of ice may be involved, hence the mechanism of hydrate formation from ice at very low temperatures may be quite different from that at higher temperatures used in this study. In either case, when hydrates form from aqueous solution or from ice crystals, the formation rate diminishes and often ceases once a protective hydrate film is formed. Vigorously shaking or stirring to crack the hydrate film and expose free water is needed in order to continue the formation process.

### 3. Experimental Procedures

Figure 1 is a schematic diagram of the experimental apparatus, which is part of an experiment originally designed to study the dissociation of hydrate cores and used in this work to examine methane hydrate formation kinetics. Details of the experimental equipment were described elsewhere [12]. In the dissociation experiments [13] powdered ice was used because the interfacial area was large and allowed hydrates to form rapidly. However, because of the powdered state, the interfacial area could not be measured. Consequently, ice was prepared differently in this work so that this variable could be measured. This will be described subsequently.

Once ice was prepared, it was placed inside the hydrate formation vessel, maintained at about  $-15^{\circ}\text{C}$  by circulating coolant through the copper cooling jacket and manifold. The vessel was then raised to  $0^{\circ}\text{C}$  where the methane and ice undergo a simultaneous phase change to form hydrates, as evidenced by a slow drop in system pressure as the hydrates formed. From the difference between the volume of the vessel and the volume of the ice in the vessel, the number of moles

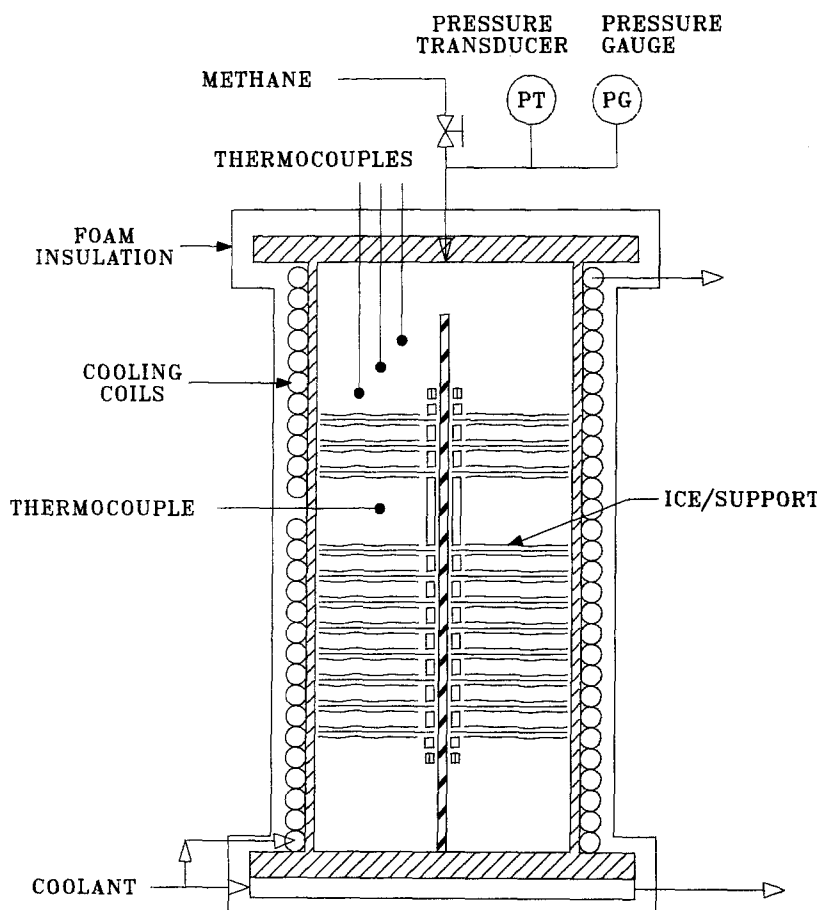


Fig. 1. Cylindrical hydrate formation vessel.

of gas (methane, in this study),  $N_g$ , could then be determined by an equation of state. The appropriate definitions are:

$$V_v = \text{volume of vessel} \quad (2)$$

$$V_i = \text{volume of ice} = (\text{mass of ice})/\text{density of ice} \quad (3)$$

$$V_g = V_v - V_i \quad (4)$$

$$N_g = PV_g/ZRT \quad (5)$$

where  $P$  is pressure,  $T$  is temperature,  $R$  is the gas constant, and  $Z$  is the compressibility factor obtained from an equation of state. As hydrates are formed, the pressure in the vessel decreases due to gas leaving the gas phase and entering the hydrate phase.

Equation 5 allows the number of moles in the gas phase to be calculated. Hence by subtracting the number of moles of gas at any time from the number originally in the vessel, the number of moles of gas in the hydrate phase is determined. By multiplying the number of moles of gas in the hydrate phase by the hydrate number (moles of water/per mole of hydrated gas), the amount of water in the hydrate phase and, by difference the amount of remaining ice can be determined. Note that the density of hydrate phase is slightly smaller, about 10%, than the density of the ice phase and as hydrates form the volume of the gas phase decreases. This volume change is taken into account when calculating the number of moles in the gas phase at any time. The hydrate number,  $\eta_h$ , is related to the ideal hydrate number,  $\eta_h^0$ , by:

$$\eta_h = \eta_h^0/\theta \quad (6)$$

where  $\theta$  is the average fractional occupancy of all hydrate cavities by gas molecules.  $\theta$  can be calculated using thermodynamic models for hydrate equilibria which have been modified and incorporated into computer programs [14]. The ideal hydrate number is defined as the hydrate number when all of the cavities are occupied, and is 5.75 for Structure I, which can be approached only in the limit of very high pressure. In this study 6.15 is used for  $\eta_h$  which, while approximate, is of sufficient accuracy for the present study.

Using this technique, the number of moles of hydrate present  $N_h$  can be calculated as a function of time. The rate of hydrate formation is then the time derivative of this function:

$$d(N_h)/d(t) = \text{rate of hydrate formation.} \quad (7)$$

The experimental set-up was connected to an IBM PC which records temperature and pressure as time progresses. A BASIC program [12] then analyzes the collected data and calculates all the pertinent variables including the mass of hydrate, the mass of unhydrated ice, the volume of gas, the number of moles of free gas, the number of moles of hydrate, and the rate of hydrate formation. This calculation can be applied to any situation in which gas and ice are present in the vessel which allows us to experiment with different geometries of ice; ice need not be powdered.

In order to provide a known interfacial area between the ice and gas during hydrate formation, a system of 304 SS disks was constructed (Figure 2). This SS rack can hold from 1 to 55 flat circular disks. The disks are 9.15 cm in diameter

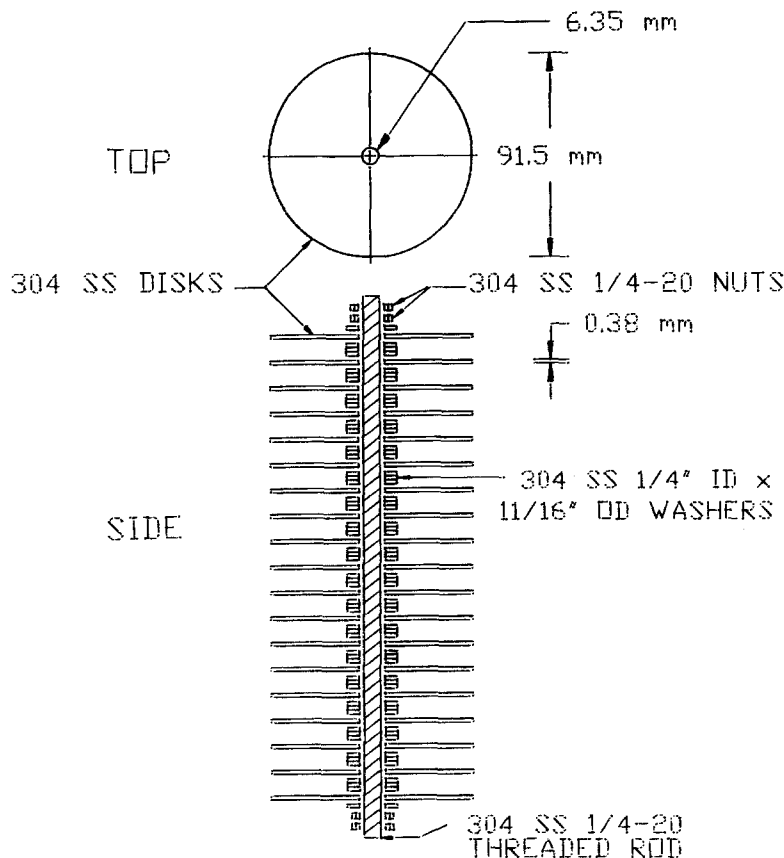


Fig. 2. Experimental rack designed to produce a well defined high gas–water interfacial surface area.

(slightly smaller than the diameter of the hydrate formation vessel) and 0.038 cm in width. The height of the rack is slightly smaller than the height of the vessel. To form hydrates the disks are coated with a thin layer of clear, crystalline ice. This is accomplished by first immersing the rack in liquid nitrogen, and then briefly in distilled water. The gas–water interfacial surface area can therefore be approximated by the total surface area of the disks.

The advantage of these experiments is that the interfacial area between the gas and ice is known so that the intrinsic rate of hydrate formation per unit surface area can be measured.

#### 4. Results and Discussion

##### 4.1. FORMATION FROM DISKS

In these experiments, hydrates would only form at a measurable rate when the initial water phase was ice (as opposed to liquid) and the temperature was raised to

a value above the ice point (0°C). Experiments were conducted with ice below 0°C and using liquid water which was slowly frozen at -1°C and in these experiments which last up to 370 h, no measurable hydrate formation took place (about 2% of the ice must be converted to hydrate to ascertain if growth was actually occurring, because of pressure fluctuations occurring with the melting or forming of ice).

Table I summarizes the experimental conditions of all runs where the temperature was raised above 0°C from approximately -10°C. Each of these runs exhibited a small pressure drop initially, due to hydrate formation, once the bulk gas temperature in the vessel reached the melting point of ice (0°C). The rate of this pressure drop, or equivalently, the rate of hydrate formation reached a maximum at an early

Table I. Experimental conditions for methane hydrate formation runs

Run No.	Int. wt. of ice (g)	Bulk gas temp. (K)	Init. gas* press. (kPa)	Final frac. ice conv.	Surface area of ice (m <sup>2</sup> )	Run time (h)
7	152.2	273.2 ± 1.5	8612	0.951	0.722	32
8	194.7	273.3 ± 1.4	6886	0.822	0.722	41
9	215.5	273.2 ± 1.4	5168	0.350	0.722	34
11	196.6	278.1 ± 0.9	8614	0.960	0.722	16
12	205.1	278.3 ± 1.0	6886	0.980	0.722	62
13	212.4	273.9 ± 1.2	8616	0.965	0.722	15
14	225.1	274.7 ± 1.4	6901	0.960	0.722	18
15	213.1	274.2 ± 1.6	5171	0.475	0.722	25
16	106.6	273.2 ± 0.3	8620	0.880	0.355	21
17	116.0	273.5 ± 0.2	6905	0.400	0.355	27
19	117.1	273.6 ± 0.2	5179	0.310	0.355	39
20	116.4	274.4 ± 0.2	8626	0.925	0.355	13
21	120.4	274.3 ± 0.2	6906	0.925	0.355	17
22	126.8	274.3 ± 0.2	5171	0.405	0.355	41
23	109.0	273.6 ± 0.9	8622	0.950	0.355	14
24	138.2	273.5 ± 0.2	10344	1.000	0.355	16
25	128.1	274.2 ± 0.5	10350	0.995	0.355	19
27	128.6	273.4 ± 0.2	12066	0.980	0.355	17
28	139.4	273.7 ± 0.4	12066	0.942	0.355	31
29	237.2	273.5 ± 0.2	8619	0.945	0.355	43
30	127.8	273.3 ± 0.3	8627	0.990	0.355	18
31	125.6	273.3 ± 0.4	7150	0.415	0.355	21
33	123.0	273.1 ± 0.2	7392	0.360	0.355	16
37	136.9	277.7 ± 0.5	6229	1.000	0.355	27
K1	128.3	273.6 ± 0.1	5836	0.450	0.355	24
K2	114.3	273.8 ± 0.2	8802	0.977	0.355	32
K3	121.9	273.7 ± 0.3	8614	0.950	0.355	21
K4	106.0	273.7 ± 0.1	6926	0.900	0.355	19
K5	117.0	273.8 ± 0.3	6922	0.945	0.355	25
K6	125.6	274.4 ± 0.4	6880	0.945	0.355	17
K7	121.8	273.6 ± 0.4	6907	0.890	0.355	37
K8	130.9	273.6 ± 0.4	6909	0.780	0.355	25
K17	104.3	273.9 ± 0.2	6906	0.990	0.276	17

\* Measured at 0°C

stage. The time elapsed before this point is referred to as the nucleation period, which is assumed to be the time required for the hydrate crystal nuclei to form on the entire surface of the disks. Because uniform growth was experimentally observed, the assumption of uniform surface nucleation is reasonable. After this period, the rate began to decay with time and this period is referred to as the crystal growth region. Table II gives the nucleation period and the corresponding maximum rate of molar ice converted per unit surface area for experimental runs using disks at temperature near 0°C. (Note that the rate of hydrate formation and the rate of ice conversion are simply related by the hydrate number). While the nucleation period can be clearly determined for higher pressure runs, this value is somewhat unclear for very low pressure runs (Group A in Table II). This can be seen in Figure 3, a plot of rate of the molar ice converted per unit surface area versus time. Figure 3 is a time derivative of Figure 4 which shows molar ice converted per unit surface area as a function of time, obtained by the technique described in the experimental procedure section. In general, higher gas pressures yield higher formation rates.

Table II. Methane hydrate formation from disks at temperatures near 0°C for different pressures

Group	Run No.	Range of init. gas press. (kPa)	Nucleation period (h)	$\frac{1}{A} \left( \frac{dN_i^*}{dt} \right)_n$ (kg-moles/m <sup>2</sup> /hr)	Rate constant $k \times 10^{-7}$ (kg-mole/m <sup>2</sup> ) <sup>2</sup> (hr <sup>-1</sup> )
A	9	5168 ~ 5836	2 $\frac{1}{3}$	0.0007	0.23
	19		1 $\frac{1}{3}$	0.0005	0.04
	K1		$\frac{5}{6}$	0.0016	0.41
B	8	6886 ~ 7392	$\frac{1}{3}$	0.0034	1.14
	17		1 $\frac{1}{6}$	0.0014	0.49
	31		1	0.0024	0.63
	33		1	0.0025	0.71
	K4		$\frac{2}{3}$	0.0079	6.58
	K7		1 $\frac{1}{3}$	0.0054	5.38
	K8		1 $\frac{1}{3}$	0.0060	5.09
C	7	8612 ~ 8627	$\frac{1}{3}$	0.0051	1.77
	16		1 $\frac{1}{3}$	0.0038	3.92
	23		1 $\frac{2}{3}$	0.0032	6.96
	29		$\frac{5}{6}$	0.0052	5.54
	30		1 $\frac{1}{6}$	0.0075	6.77
	K3		$\frac{1}{2}$	0.0134	14.79
D	24	10344 ~ 12066	1 $\frac{1}{2}$	0.0043	6.84
	25		1 $\frac{5}{6}$	0.037	4.94
	27		$\frac{1}{2}$	0.0079	5.63
	28		$\frac{1}{2}$	0.0050	7.15

\*  $N_i$  is the moles of ice converted to hydrate.

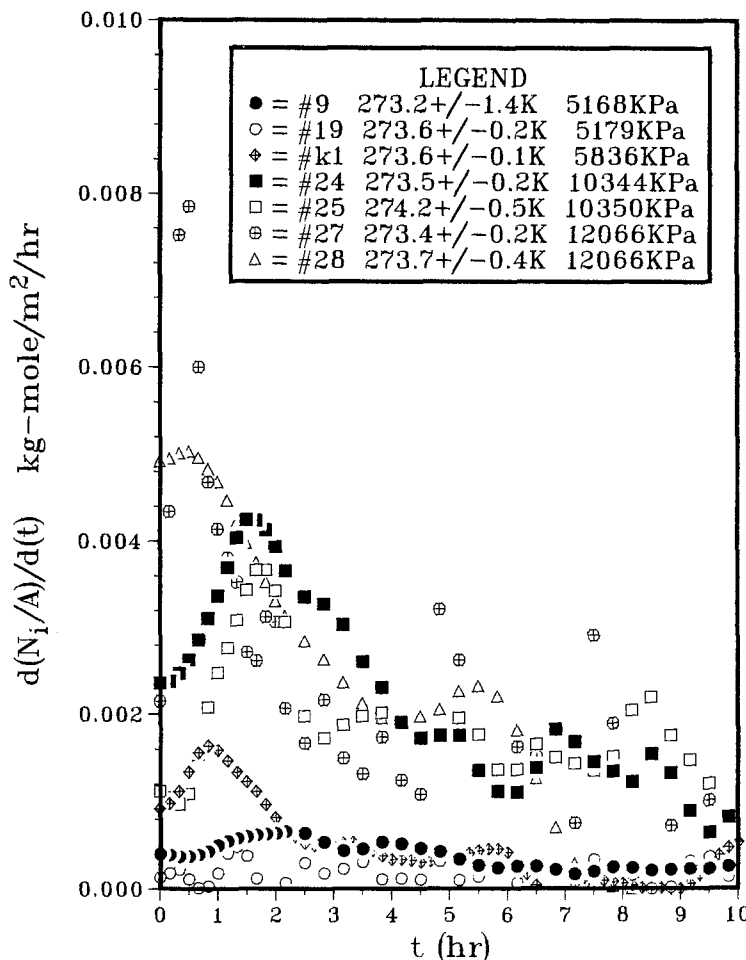


Fig. 3. Rate of molar ice conversion per unit surface area versus elapsed time.

The effect of pressure on hydrate growth is due to several reasons. First the equilibrium water content (concentration of water) in the gas phase is increased at higher pressures. Second, the denser gas is a better conductor of heat and can thus remove the heat of formation more easily. Third, at higher pressures, the hydrate is stable at higher temperatures and the heat of hydrate formation can be partially absorbed as sensible heat. On a macroscopic level, higher pressures produce a greater temperature driving force for hydrate formation. Experimental runs with a 'K' in the run number used a slight variation in experimental techniques. Normally, the vessel was pressurized only after inserting the disks and allowing them to cool for several hours; in the K-runs the system was pressurized as soon as the disks were inserted. This probably resulted in some prenucleation from moisture which may have been condensed on the surface, thus a higher ice conversion rate was obtained for 'K' runs. It can be observed in Table II that the maximum ice conversion rate

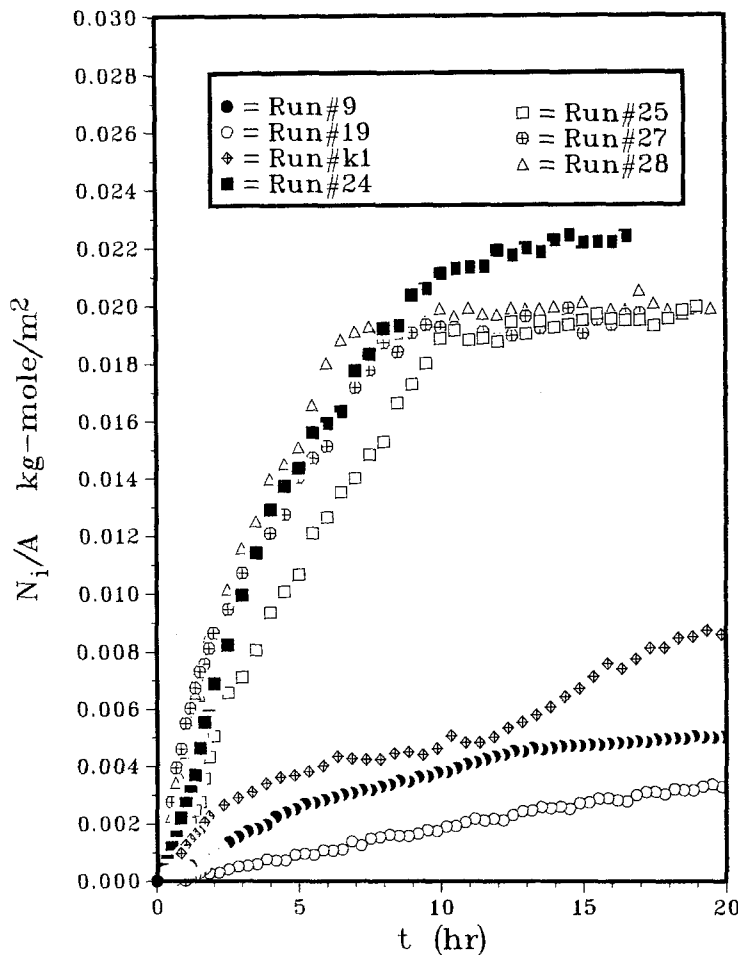


Fig. 4. Molar ice conversion per unit surface area versus elapsed time.

per unit surface area is generally increased with an increase in pressure but the  $K$ -runs have different absolute rates due to differences in nucleation. The nucleation period was expected to decrease with pressure, but does not appear to do so (Table II); two facts account for this: (1) nucleation is largely affected by the process of warming up the vessel to the ice point, which varies slightly from run to run due to human control; (2) the beginning of the nucleation period (the point that pressure starts to drop) is difficult to determine precisely.

Based upon the observation that the growth rate decays with time, a kinetic model was proposed which assumes that the growth rate is inversely proportional to the thickness of the hydrate layer on the ice.

$$\frac{1}{A} \frac{dN_h}{dt} = \frac{k}{(N_h/A)} \quad (8)$$

or

$$\left(\frac{N_h}{A}\right)^2 - \left(\frac{N_h}{A}\right)_n^2 = 2k(t - t_n) \quad (9)$$

where the subscript  $n$  denotes the end of the nucleation period or the beginning of the growth period,  $A$  is the gas-water interfacial surface area,  $k$  is the crystal growth rate constant, and  $t$  is the total time elapsed. The equation is valid for times greater than  $t_n$ , the time of the nucleation period.

Figure 5 shows a plot of  $(N_h/A)^2 - (N_h/A)_n^2$  versus growth time  $(t - t_n)$  for a typical run. The growth rate constant,  $k$ , is then determined as half of the slope of the straight line drawn through the data. The hydrate growth rate constants,  $k$ , were found to be  $0.1 \sim 10 \times 10^{-7}$  (kg-mole/m<sup>2</sup>)<sup>2</sup>/h for formation temperatures near 0°C

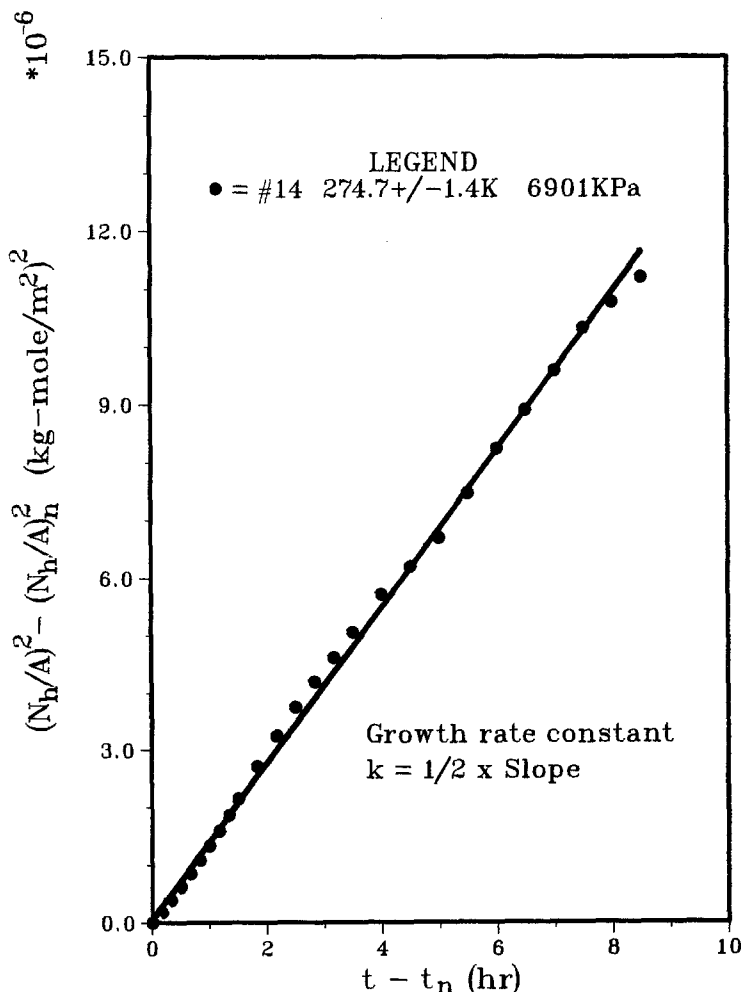


Fig. 5. Proposed kinetic model for hydrate crystal growth. Growth rate constant  $k$  equals half value of the slope of the straight line.

and are given in Table II. In general,  $k$  increases as system pressure increases; this effect is larger at lower pressure (Group B to Group C,  $\sim 7000$  kPa to  $\sim 8600$  kPa) but is insignificant at higher pressures (Group C to Group D, pressure greater than 10 000 kPa). The same trend was observed for the  $K$ -runs.

At lower pressures, temperature also has an effect on the hydrate formation rate in that higher temperatures give higher formation rates for the same gas pressures (Figure 6). It is hypothesized that the temperature effect is related to the rate of ice melting. Apparently, at low pressures the hydrate formation is limited by the rate of ice melting and higher temperatures allow the ice to melt more rapidly thus give higher formation rates.

Upon examining the ice rack after each experiment the methane hydrate crystals typically appeared as a thick, opaque white film which grew perpendicular to the surface of the disks and filled the space between the disks (Figure 7). Close inspection of the methane hydrate films shows it to be a dense array of straight,

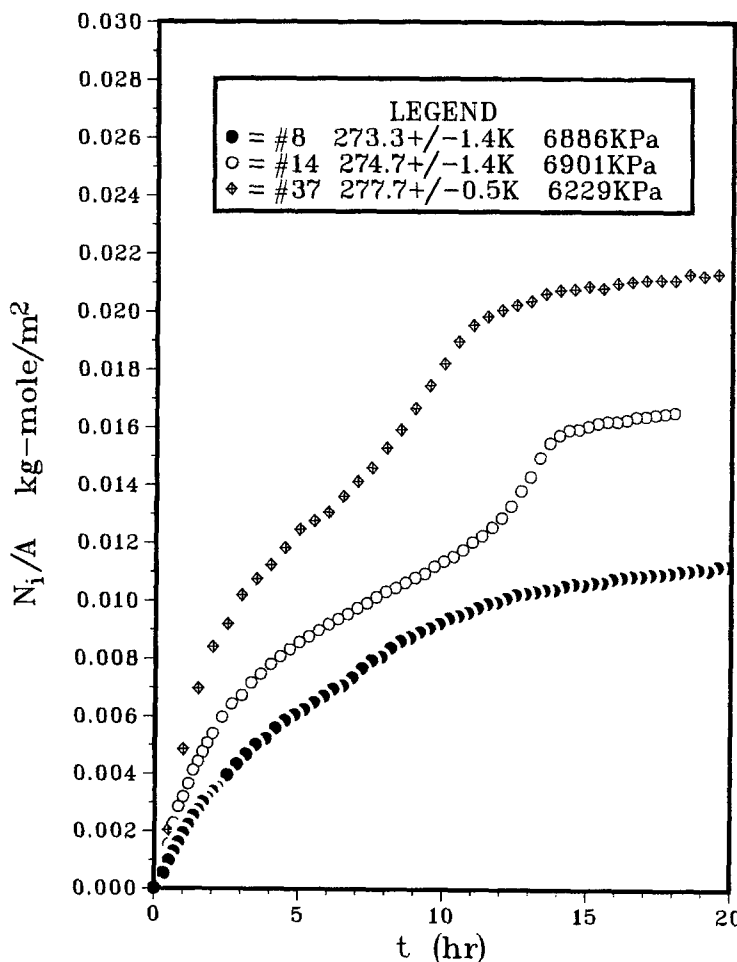


Fig. 6. Effect of temperature on hydrate formation rate.



Fig. 7. Methane hydrate crystals formed from disks.

vertical fibers. Since hydrates are only slightly less dense than ice, their ability to fill the voids between the disks means that the hydrates formed were very bulky and contained many voids.

#### 4.2. PROPOSED MECHANISM

Upon raising the temperature of the ice to its melting point, two distinct and measurable periods of methane hydrate formation were observed, provided the pressure driving force was large enough. During the initial or 'nucleation' period, which typically lasted from 0.5 to 3 h, the formation rate increased with time and quickly reached a maximum value. This was followed by the 'growth' period, during which the formation rate decayed with time until no more ice remained on the disks.

The mechanism of hydrate formation during the 'nucleation' period is similar in nature to hydrate crystal nucleation on the surface of water or ice as described by Makogon [1]. At the melting surface, the water molecules are more mobile and are able to interact with methane gas molecules and rearrange to form individual Structure I hydrate crystal lattices at locations referred to as nucleation sites. However, since both ice and hydrates are tetrahedrally bonded, the ice structure serves as a molecular template for hydrate formation. To form stable nuclei a certain degree of intermediate range structure is needed. Perhaps one coordination number (20 water molecules) must be organized into a structure. The crystalline nature of both ice and hydrate structures allows ice to more readily supply this

structure than liquid water. Additionally, the activation energy for reorganizing melting ice into hydrate is probably less than the activation energy required to reorganize ice into liquid water. Only those sites with crystals larger than a certain critical size will remain thermodynamically stable, with smaller crystals disappearing at the expense of larger ones. The agglomeration of small hydrate crystals continues until active nucleation sites cover nearly the entire ice surface.

During the 'growth' period, crystals grow only from the existing sites. The unidirectional nature of the crystal growth observed in this work indicates that a large number of closely and uniformly spaced nucleation sites were formed on the disk surface originally. The growth of hydrate crystals could continue in two ways, first, methane molecules could diffuse through the growing hydrate film and combine with free melted, water molecules. This mechanism is the 'volume-diffusion' mechanism proposed by Makogon [1]. Second, water molecules produced during melting reach the external crystal surface through gravity, capillary action, and vapor phase diffusion. In both models, one of the species, methane or water, must diffuse through or around the hydrate layer. The dendritic nature of the growth appears to support the latter mechanism.

## 5. Conclusions

The hydrate formation appears to be an interfacial phenomena. Experiments with well defined gas–water interfacial surface area were developed to study methane hydrate formation rates. Rates of hydrate crystal growth were found to be inversely proportional to the thickness of the hydrate zone. The following conclusions can be drawn from this study.

1. The process of hydrate formation exhibits two distinct periods – 'nucleation' and 'growth'. Nucleation takes place only at the gas–water interfacial surface and the method of nucleation affects the ultimate growth rate.
2. Melting ice plays an important role in hydrate crystallization. After the ice melts, the water retains some of its structure in the liquid phase and this structure serves as a template for hydrate nuclei formation.
3. Once hydrates are nucleated, growth is possible from liquid water or from melting ice, or from the vapor as long as the gas and water molecules are available to the growth surface. Melting ice has the advantage that the energy produced during hydrate formation can be largely absorbed by melting ice. However, if heat transfer were not a limitation, hydrate growth should be faster from liquid water. Growth rates are primarily determined by the rate of the supply of hydrate forming species to the growth surface and the rate of the removal of the heat of formation from the forming surface.
4. Increasing the pressure increases the rate of hydrate formation.
5. While the results are well described by the proposed model, the model constant 'k' depends upon the experimental system and is not a generalizable parameter.

## Acknowledgement

The authors acknowledge the support of the department of energy under grant DE-AC21-85-MC2221.

## References

1. Y. F. Makogon: *Hydrates of Natural Gas*, W. J. Cielewicz Translation, PennWell Publishing, Tulsa, Oklahoma, 1981.
2. J. L. Cox (ed.): *Natural Gas Hydrates: Properties, Occurrence and Recovery*, Butterworth Publisher, Boston, Massachusetts, 1983.
3. D. W. Davidson: *Clathrate Hydrates* (Water: A Comprehensive Treatise Vol. 2, ed. F. Franks), Chapter 3, Plenum, New York, 1973.
4. J. Finjord: *Hydrates of Natural Gas, A State-of-the Art Study with Emphasis on Fundamental Properties*, T. 11/83, Rogaland Research Institute, Stavanger, Norway, 1983.
5. G. D. Holder, S. P. Zetts, and N. Pradhan: *Rev. Chem. Eng.* **5**, 1 (1988).
6. R. M. Barrer and D. J. Ruzicka: *Trans. Faraday Soc.* **58**, 2262 (1962).
7. A. Vysniauskas and P. R. Bishnoi: *Chem. Eng. Sci.* **38**, 1061 (1983).
8. A. Vysniauskas and P. R. Bishnoi: *Chem. Eng. Sci.* **40**, 299 (1985).
9. B. B. Maini and P. R. Bishnoi: *Chem. Eng. Sci.* **36**, 183 (1981).
10. R. M. Barrer and A. V. J. Edge: *Proc. Royal Soc. London A* **300**, 1 (1967).
11. B. J. Falabella: *A Study of Natural Gas Hydrates*, Ph.D. Diss., Univ. of Massachusetts, 1975.
12. D. A. Wright: *A Kinetic Study of Methane Hydrate Formation from Ice*, M.S. Thesis, Univ. of Pittsburgh, 1985.
13. V. A. Kamath and G. D. Holder: *AIChE Journal* **33**, 347 (1987).
14. V. T. John and G. D. Holder: *AIChE Journal* **31**, 252 (1985).